Applied Catalysis B: Environmental 192 (2016) 88–92

Contents lists available at ScienceDirect

Applied Catalysis B: Environmental

journal homepage: www.elsevier.com/locate/apcatb

Application of picene thin-film semiconductor as a photocatalyst for photocatalytic hydrogen formation from water

Atsushi Okemoto[a], Kensuke Kishishita[a], Sho Maeda[a], Shin Gohda[b], Masahiro Misaki[a,c], Yasuko Koshiba[a,c], Kenji Ishida[a,c], Takafumi Horie[a,c], Keita Taniya[a,c], Yuichi Ichihashi[a,c,*], Satoru Nishiyama[a,c]

[a] Department of Chemical Science and Engineering, Graduate School of Engineering, Kobe University, Rokkodai, Nada, Kobe 657-8501, Japan
[b] Nard Institute, Ltd., Nishinagasucho, Amagasaki 660-0805, Japan
[c] Center for Membrane and Film Technology, Graduate School of Engineering, Kobe University, Rokkodai, Nada, Kobe 657-8501, Japan

ARTICLE INFO

Article history:
Received 1 March 2016
Received in revised form 11 March 2016
Accepted 12 March 2016
Available online 18 March 2016

Keywords:
Photocatalysis
Organic semiconductor
Hydrogen formation
Picene

ABSTRACT

Interesting photocatalytic properties of a picene thin film on quartz (PTF/Q) have been demonstrated for photocatalytic hydrogen formation from water using several sacrificial agents. Hydrogen is produced in the presence of PTF/Q catalysts under light irradiation, indicating that PTF/Q works as a photocatalyst. The catalyst retains its activity under light irradiation and addition of sacrificial agents enhanced the rate of photocatalytic hydrogen formation from water, similar to the condition when a traditional inorganic photocatalyst is used. Moreover, PTF/Q catalysts comprising picene films of different thickness have been fabricated, and PTF/Q with the thinnest film (50 nm) exhibits the highest activity for hydrogen formation. X-ray diffraction patterns show that the picene crystals are vertically aligned on the surface of the quartz sheet, and that PTF/Q with the thinnest film has a nonuniform film phase. The difference of picene thin-film surface in morphology probably influences the photocatalytic activity. The absorption edge and optical gap energies of the prepared PTF/Q catalyst are determined and the optical gap of the picene film is calculated to be 3.2 eV.

1. Introduction

Hydrogen has attracted attention as a potential environmentally clean energy fuel, as it can help in overcoming the side effects of greenhouse gas emission and realising a sustainable society [1–3]. In this regard, photocatalytic routes to hydrogen production, in particular the photodecomposition of water, have been the topic of extensive research [4–7]. Many researchers have reported photocatalytic reactions over inorganic semiconductors, with particular focus on enhancing their photocatalytic activity towards the water decomposition reaction. Sacrificial organic electron donors such as alcohols, organic acids, and hydrocarbons often have been employed as hole scavengers to enhance the efficiency of the photodecomposition of water [8–11]. To date, however, most of the photocatalysts used for the aforementioned reaction are inorganic semiconductors with or without sacrificial agents or additives. Inorganic semiconductors are disadvantageous in that they require a high-temperature annealing step to ensure high performance. It is not easy to induce energy level changes because they have their individual energy levels associated with strong crystal structures. Many studies have investigated inorganic photocatalysts by arbitrarily modifying energy levels. In recent times, organic molecules as photocatalysts are also being increasingly investigated to control the structures and energy levels through band gap engineering approaches such as inorganic-organic hybrids and photo-active MOFs [12]. Here, we show that simple organic semiconductors can function as metal-free organic photocatalysts, which can easily change and control their optical absorption property for extracting hydrogen from water. Organic semiconductors have been used in new applications to replace inorganic semiconductors in various fields of late years. Organic semiconductor crystals have been extensively researched because of their high purity, long-range order, and unique optical structures. Consequently, there has been rapid development in organic electronics based on these crystals (organic light emitting diodes (OLEDs), integrated photonic circuits, and photovoltaic cells), as they have advantageous over traditional silicon-based semiconductor devices [13–18]. Additionally, the

* Corresponding author at: Department of Chemical Science and Engineering, Graduate School of Engineering, Kobe University, 1-1 Rokkodai, Nada, Kobe 657-8501, Japan.
E-mail address: ichiy@kobe-u.ac.jp (Y. Ichihashi).

http://dx.doi.org/10.1016/j.apcatb.2016.03.028
0926-3373/

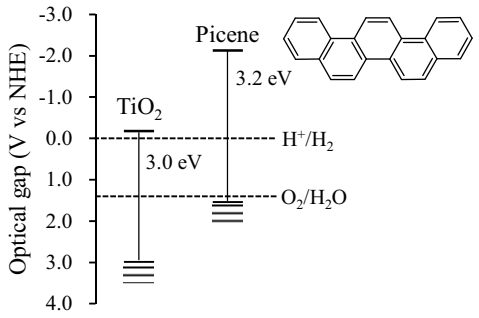

Fig. 1. Energy level diagram of picene and TiO_2.

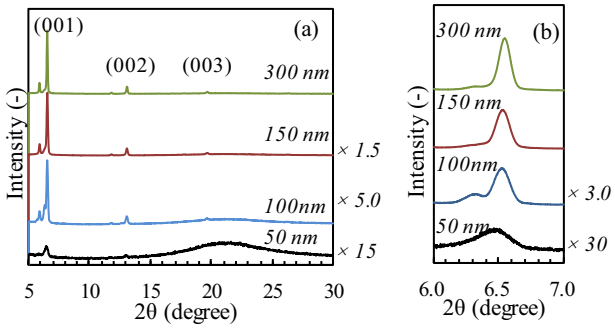

Fig. 2. XRD patterns of PTF/Q of different film thickness; (a) the wide scans in the region 5.0°–30.0°, (b) the narrow scans in the region 6.0°–7.0°.

unique mechanical properties of organic semiconductors allow for the fabrication of flexible electronic devices such as mobile appliances and solar cells, whose market position has been strengthened because of their high mechanical flexibility and ease of mass production [19,20]. However, applications of organic semiconductors have been limited to the field of electronics. The photocatalytic properties of organic semiconductors, which differ from those of traditional inorganic semiconductors in terms of molecular orientation, intermolecular interactions, and wavelength selectivity, have not been investigated in detail, even though organic semiconductors are expected to many unique photocatalytic properties. Consequently, there are only a few reports on the use of organic semiconductors as photocatalysts [21,22]. In this study, we used a photocatalytic system featuring an organic thin-film semiconductor for hydrogen evolution from water. Picene was chosen as the organic semiconductor because its band gap is close to the energy level of typical inorganic semiconductors, such as TiO_2, which is required for the decomposition of water, as shown in Fig. 1 [23,24]. Picene thin-film catalysts were prepared by thermal evaporation under vacuum, and the photocatalytic decomposition of water was performed in the presence of several sacrificial agents to evaluate the photocatalytic performance of the picene catalysts. The reaction was also performed using picene catalysts with different film thickness to investigate the influence of the film-forming state of picene crystal on the photocatalytic performance.

2. Experimental

2.1. Catalyst preparation

Pure picene powder was obtained from NARD Institute, Ltd., Japan. Picene film was deposited on a quartz glass substrate by thermal evaporation under vacuum using a SANYU SVC-700TM system. Before deposition, the substrate (quartz size; 10 mm × 40 mm × 0.5 mm) was cleaned using acetone in an ultrasonic bath, and dried at 333 K. The substrate was then placed in the substrate holder of the deposition system, which was positioned approximately 25 cm above a molybdenum boat containing the picene powder. The holder and boat were placed in a vacuum chamber that was pumped down to a base pressure of 10^{-4} Torr by using a diffusion pump. Subsequently, the molybdenum boat was heated by electric current of ~10 A to sublime picene, and the picene film was deposited on the substrate at a deposition rate of 0.2 nm s^{-1}.

2.2. Photocatalytic reaction for hydrogen formation from water

Water decomposition was carried out in a batch reactor system. The prepared catalyst (picene thin film/quartz; PTF/Q) and 5.0 mL aqueous urea solution (0.3 M) were placed in a 7.8 mL cylindrical quartz reactor. Dry argon gas was bubbled through the solution for 15 min to ensure complete removal of air, and then the entire reactor was purged with argon. The rector was placed at 5 cm from the window of lamp. Light irradiation was performed by using a 500 W Xe lamp (USHIO, SX-UI501XQ) equipped with a 250 nm cut-off filter (HOYA UV-25) which was positioned at a distance of 1 cm from the window of the lamp. After the reaction was complete, the vapour-phase components were withdrawn by a syringe and analysed by gas chromatography (Shimadzu GC-8A) using a thermal conductivity detector (containing molecular sieve 13x column and Ar carrier).

2.3. Characterisation

The structure and crystallinity of the thin film were characterised by X-ray diffraction (XRD) using a RIGAKU RINT2100 system with Cu Kα (λ = 1.5406 Å) radiation. Standard scans were acquired from 5° to 30° (2θ) at a step size of 0.020° (2θ) and a dwell time of 1 s per step. Fine scans were acquired from 6° to 7° (2θ) at a step size of 0.002° (2θ) and a dwell time of 1 s per step. UV–vis spectra was recorded using a UV–vis absorption spectrophotometer (Hitachi U-3210D) in the region 200–800 nm at a step size of 1 nm. The optical gap was calculated from the absorption edge of the UV–vis absorption spectrum using the formula ΔE_{opt} (eV) = 1237.5/λ (in nm).

3. Results and discussion

3.1. Structure of picene thin-film photocatalysts

The structural characterisation of PTF/Q of different film thickness was performed based on X-ray diffraction pattern measured at 298 K. The XRD patterns of the PTF/Q catalysts are shown in Fig. 2. Diffraction lines in Fig. 2(a) ascribable to (001), (002), (003), and (004) reflections are observed, indicating highly oriented single crystal growth of the picene layer with vertical periodicity of 13.5 Å [25–27]. These diffraction patterns give an interphase distance with *c* axis length of 13.5 Å, which corresponds to the slightly tilted phase of picene crystal on a substrate. Picene clusters form a highly ordered and crystalline thin film that is nearly identical to those observed for the *c* axis in single crystals, as shown by the (00l) reflections [27]. These reflections indicate that the *a*,*b* planes of the grains are oriented parallel to the substrate surface. Hence, such Bragg reflections are attributed to the vertical orientation of most picene molecules on the quartz substrate [28] (see Fig. S1 in Supporting Information). Fig. 2(b) shows the fine XRD scans in the region 6.0°–7.0°. All diffractions in Fig. 2(b) show two peaks, located at 6.30° and 6.54°, which are assigned to the vertical periodicity of 14.0 Å (Phase 1) and the slightly tilted crystalline phase of 13.5 Å (Phase 2), respectively [29]. The peak profiles were analysed using pseudo Voigt functions (see Fig. S2 in Supporting

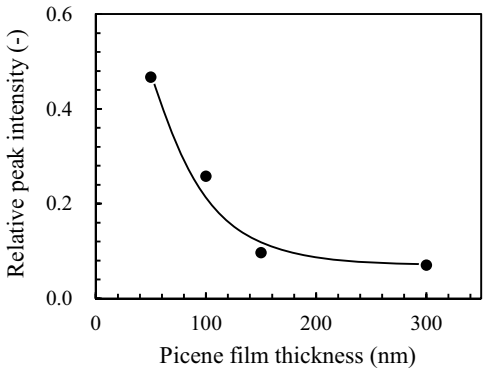

Fig. 3. The relative peak intensity of PTF/Q with different film thickness of the picene film, which is calculated based on the XRD peak intensity of Phase 1 divided by that of Phase 2.

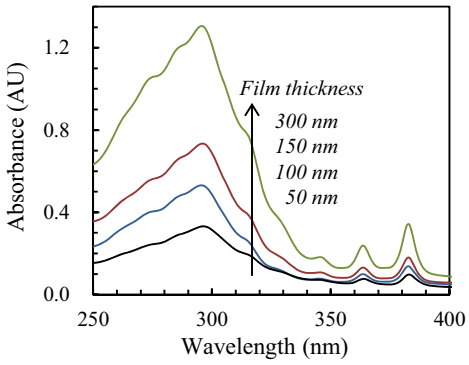

Fig. 4. UV–vis absorption spectra of PTF/Q of different film thickness (50–300 nm).

Information), and an asymmetry peak was detected towards lower angles. The fitted pseudo Voigt profiles give the relative peak intensity as a parameter of non-uniformity of the crystal phase, which is a ratio calculated using the peak intensity of Phase 1 divided by that of Phase 2. The relative peak intensities of PTF/Q of different film thickness are shown in Fig. 3. PTF/Q with a film thickness of 50 nm has the highest relative peak intensity, and the relative peak intensity drastically decreases as the film thickness of picene increases. An increase in the relative peak intensity indicates unevenness of the picene crystal phase due to the formation of polycrystalline picene film mixed with two phases. Thus, it is estimated that PTF/Q with the lower picene crystal thickness has a rough surface.

The UV–vis absorption spectra of PTF/Q of different film thickness are shown in Fig. 4. Absorption peaks attributed to π-π* transitions of picene molecules are observed in the region 340–400 nm [30]. Although PTF/Q containing a thicker picene crystal is able to absorb a larger amount of light, film thickness has no influence on the absorption edge. The absorption edge of all samples is 383 nm, and the optical gap is calculated to be 3.2 eV by the formula ΔE_{opt} (eV) = 1237.5/λ (in nm); the calculated value is consistent with the literature data [13,31]. As this catalyst exhibits absorption over a wide range in the ultraviolet region, it is expected to work as a photocatalyst.

3.2. Photocatalytic tests

Table 1 shows the results for hydrogen production over PTF/Q with film thickness of 300 nm via the photodecomposition of water in the presence of several sacrificial agents for 8 h reaction time. Hydrogen production is not observed over a pure quartz substrate (entry 1), and without light irradiation (entry 2). These results indicate that hydrogen is not generated through the direct

Table 1
Hydrogen yield in the photodecomposition of water over PTF/Q (film thickness: 300 nm) in the presence of several sacrificial agents for 8 h of a reaction time.

Entry	Catalyst	Reactant	Light	Yield of hydrogen (μ mol/m^2)
1	Quartz	water + urea	on	0.0
2	PTF/Q	water + urea	off	0.0
3	PTF/Q	water	on	10.0
4	PTF/Q	water + urea	on	27.0
5	PTF/Q	water + methanol	on	1084.0
6	PTF/Q	water + ethanol	on	738.0
7	PTF/Q	water + formic acid	on	3915.0
8	PTF/Q	water + lactic acid	on	604.0

Reaction conditions: Water with several sacrificial agents (4.8 mol/L), Picene thin-film catalyst on a quartz (PTF/Q), room temperature.

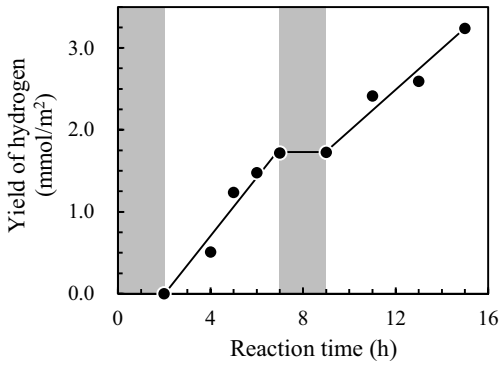

Fig. 5. Hydrogen evolution from water with formic acid over PTF/Q (film thickness: 50 nm) with and without light irradiation.

photodecomposition of picene or the chemical reaction of sacrificial agents on the picene film. Light irradiation onto PTF/Q in pure water leads to the slight formation of hydrogen (10 μmol/m^2, entry 3), indicating that the photocatalytic production of hydrogen from water proceeds over PTF/Q. The addition of sacrificial agents to water accelerates hydrogen production (entry 4–8), especially in the presence of formic acid, with the highest yield of hydrogen obtained as 3915.0 μ mol/m^2 (entry 7). It is confirmed that sacrificial agents efficiently enhance consumption of holes. The results indicate that both PTF/Q and light irradiation are indispensable for the photodecomposition of water.

Fig. 5 shows the time profile of hydrogen evolution over PTF/Q with film thickness of 300 nm. No formation of hydrogen is observed in the reaction without light irradiation; further, it is confirmed that PTF/Q does not undergo photodegradation, because hydrogen production increases linearly with time. The total evolution of hydrogen is 1.30 μmol in this reaction, exceeding the amount of hydrogen included in picene (8.84×10^{-2} μmol) deposited on the quartz. It is suggested that picene hardly decomposes during the reaction and hydrogen is formed from water decomposition. These were also supported by the formation of D_2 from D_2O from mass spectroscopy. Repeated tests of the used PTF/Q were carried out, and the results are shown in Fig. 6. The used catalyst has almost the same rate of hydrogen production as the fresh one and PTF/Q retains its activity after 16 h of repeated runs. No change of XRD patterns and UV–vis absorption spectra of PTF/Q catalysts after the reaction was observed, indicating that the structure of picene thin-film was maintained under light irradiation. The reusability study shows that the PTF/Q structure was stable throughout the reaction.

From the above mentioned observations, it can be concluded that the organic semiconductor consisting of a picene crystal film can effectively catalyse the photodecomposition of water to hydrogen. The photocatalytic activity of PTF/Q of different film thickness was also evaluated by the photodecomposition of water

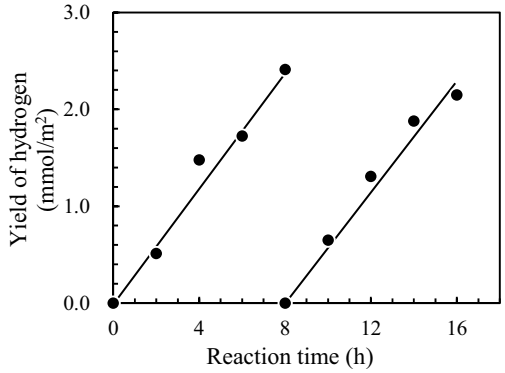

Fig. 6. Repeated tests for photocatalytic hydrogen formation from water with formic acid over PTF/Q with film thickness of 50 nm.

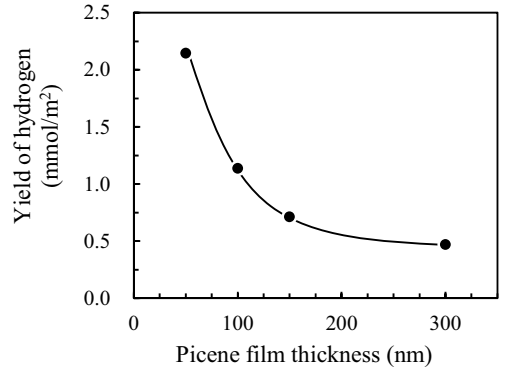

Fig. 7. Hydrogen yield in the photodecomposition of water with formic acid over PTF/Q with different thickness of the picene film for 10 h of a reaction time.

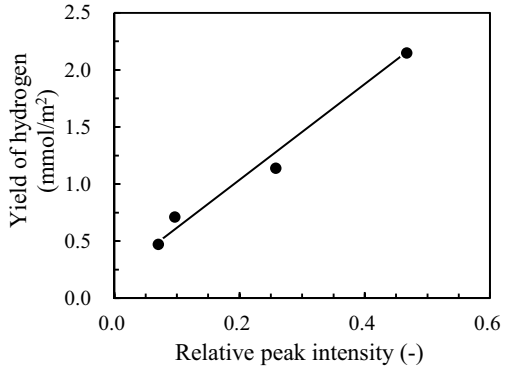

Fig. 8. The dependence of hydrogen yield on the relative peak intensity based on XRD measurements.

with formic acid for 10 h (see Fig. 7). PTF/Q with the thinnest film (50 nm) exhibits the highest activity for hydrogen formation (2.15 mmol/m^2). A decrease in hydrogen yield was clearly observed with an increase in picene film thickness on the quartz, despite the fact that the catalysts containing thicker picene films show more efficient absorption in the UV–vis region. The excellent activity observed for PTF/Q with film thickness of 50 nm is considered to be attributed to an advantage in the crystal structure. As described above, it is suggested that PTF/Q with lower picene crystal thickness has a rough surface since PTF/Q with film thickness of 50 nm has the highest relative peak intensity based on the XRD measurements (see Fig. 3). The relationship between the hydrogen yield and relative peak intensity based on diffraction patterns is shown in Fig. 8. The catalyst with the highest relative peak intensity shows the best activity (2.15 mmol/m^2), and there is a proportionally strong dependence between the hydrogen yield and relative peak intensity. A decrease in the relative peak intensity indicates that PTF/Q comprises a highly crystallised single crystal of Phase 2 and a uniform catalyst surface. A highly crystallised phase shows less activity due to a uniform surface and a smooth specific surface area. In contrast to a highly crystallised film phase, a microcrystalline grain of picene shows high activity, probably because it has a broad contact area of rough surfaces and numerous active sites. Therefore, it is suggested that the picene crystal phase of Phase 1 is the major active species and PTF/Q with a film thickness of 50 nm has a rough surface and numerous active sites, and hence, it shows excellent photocatalytic activity for hydrogen formation. The result indicates that the control of the surface morphology is very important to further improve the performance of PTF/Q in the photocatalytic process.

4. Conclusions

It was found that PTF/Q showed photocatalytic activity for the decomposition of water in the presence of several sacrificial agents. PTF/Q containing a thinner film showed the best photocatalytic activity due to the roughness of the catalyst surface, based on the analysis of XRD measurements. Diffraction patterns also revealed that the picene crystals were highly oriented, in a vertical manner, on the surface of the quartz substrate. UV–vis absorption spectra revealed that the optical gap of the catalyst was equivalent to 3.2 eV and picene showed electron transitions from a π-bonding orbital to an antibonding π orbital* in the 340–400 nm region. It was speculated that the excited electrons by π-π* transitions of picene molecules probably contributed to this photocatalytic reaction. The presented work successfully demonstrated the utility of organic semiconductors for the photocatalysis. The results of this study are expected to contribute to the design of efficient and sustainable photocatalytic systems using organic semiconductor catalysts for a wide variety of photocatalytic reactions. It seems necessary to investigate photo-active sites in organic semiconductors and the reaction mechanism, and also to design surface morphology of films, including photocatalyst components and their specific surface area, in the future.

Appendix A. Supplementary data

Supplementary data associated with this article can be found, in the online version, at http://dx.doi.org/10.1016/j.apcatb.2016.03.028.

References

[1] T. Bak, J. Nowotny, M. Rekas, C.C. Sorrell, Int. J. Hydrogen Energy 27 (2002) 991–1022.
[2] M. Pumera, Energy Environ. Sci. 4 (2011) 668–674.
[3] A. Steinfeld, Sol. Energy 78 (2005) 603–615.
[4] R. Dholam, N. Patel, M. Adami, A. Miotello, Int. J. Hydrogen Energy 34 (2009) 5337–5346.
[5] A. Kudo, Y. Misekia, Chem. Soc. Rev. 38 (2009) 253–278.
[6] K. Obata, K. Kishishita, A. Okemoto, K. Taniya, Y. Ichihashi, S. Nishiyama, Appl. Catal. B Environ. 160–161 (2014) 200–203.
[7] R. Abe, J. Photochem. Photobiol. C Photochem. Rev. 11 (2010) 179–209.
[8] A. Kudo, Y. Misekia, Chem. Soc. Rev. 38 (2009) 253–278.
[9] T. Sreethawong, Y. Suzuki, S. Yoshikawa, Int. J. Hydrogen Energy 30 (2005) 1053–1062.
[10] G.L. Chiarello, M.H. Aguirre, E. Selli, J. Catal. 273 (2010) 182–190.
[11] K. Shimura, H. Kawai, T. Yoshida, H. Yoshida, ACS Catal. 2 (2012) 2126–2134.
[12] T. Toyao, N. Ueno, K. Miyahara, Y. Matsui, T.H. Kim, Y. Horiuchi, H. Ikeda, M. Matsuoka, Chem. Commun. 51 (2015) 16103–16106.
[13] M. Grätzel, Nature 414 (2001) 338–344.
[14] A.P. Alivisatos, J. Phys. Chem. 100 (1996) 13226–13239.
[15] G. Chen, H. Sasabe, T. Igarashi, Z. Hong, J. Kido, J. Mater. Chem. A 3 (2015) 14517–14534.
[16] J.Y. Kim, T. Yasuda, Y.S. Yang, C. Adachi, Adv. Mater. 25 (2013) 2666–2671.

[17] Y. Jouane, S. Colis, G. Schmerber, A. Dinia, P. Lévêque, T. Heiser, Y.A. Chapuis, Org. Electron. 14 (2013) 1861–1868.
[18] J.A. Merlo, C.R. Newman, C.P. Gerlach, T.W. Kelley, D.V. Muyres, S.E. Fritz, M.F. Toney, C.D. Frisbie, J. Am. Chem. Soc. 127 (2005) 3997–4009.
[19] D.L. Talavera, G. Nofuentes, J. Aguilera, M. Fuentes, Renew. Sustainable Energy Rev. 11 (2007) 447–466.
[20] C.D. Dimitrakopoulos, P.R.L. Malenfant, Adv. Mater. 14 (2002) 99–117.
[21] K. Nagai, T. Abe, Y. Kaneyasu, Y. Yasuda, I. Kimishima, T. Iyoda, H. Imaya, ChemSusChem 4 (2011) 727–730.
[22] T. Abe, Y. Tanno, N. Taira, K. Nagai, RSC Adv. 5 (2015) 46325.
[23] H. Okamoto, N. Kawasaki, Y. Kaji, Y. Kubozono, A. Fujiwara, M. Yamaji, J. Am. Chem. Soc. 130 (2008) 10470.
[24] S. Trasatti, Pure Appl. Chem. 58 (1986) 955–966.
[25] S. Gottardi, T. Toccoli, S. Iannotta, P. Bettotti, A. Cassinese, M. Barra, L. Ricciotti, Y. Kubozono, J. Phys. Chem. C 116 (2012) 24503–24511.
[26] A.K. Diallo, R. Kurihara, N. Yoshimoto, C.V. Ackermann, Appl. Surf. Sci. 314 (2014) 704–710.
[27] T. Djuric, T. Ules, H.G. Flesch, H. Plank, Q. Shen, C. Teichert, R. Resel, M.G. Ramsey, Cryst. Growth Des. 11 (2011) 1015–1020.
[28] Y. Kubozono, H. Goto, T. Jabuchi, T. Yokoya, T. Kambe, Y. Sakai, M. Izumi, L. Zheng, S. Hamao, H.L.T. Nguyen, M. Sakata, T. Kagayama, K. Shimizu, Physica C 514 (2015) 199–205.
[29] I.P.M. Bouchoms, W.A. Schoonveld, J. Vrijimoeth, T.M. Klapwiji, Synth. Met. 104 (1999) 175.
[30] S. Fanetti, M. Citroni, R. Bini, L. Malavasi, G.A. Artioli, P. Postorino, J. Chem. Phys. 137 (2012) 224506.
[31] Q. Xin, S. Duhm, F. Bussolotti, K. Akaike, Y. Kubozono, H. Aoki, T. Kosugi, S. Kera, N. Ueno, Phys. Rev. Lett. 108 (2012) 226401.